

Conformational Fluctuations and Large Fluorescence Spectral Diffusion in Conjugated Polymer Single Chains at Low Temperatures

T. Pullerits, O. Mirzov, and I. G. Scheblykin*

Chemical Physics, Lund University, P.O. Box 124, 22100 Lund, Sweden

Received: April 27, 2005; In Final Form: August 8, 2005

The fluorescence of single chains of the conductive polymer poly[2-methoxy-5-(2'-ethylhexyloxy)-1,4-phenylene vinylene] (MEH-PPV) was studied by means of single-molecule spectroscopy at 15 K. MEH-PPV was deposited onto a surface from a toluene solution and covered with a polymer cap layer of poly(vinyl alcohol) spin-coated from an aqueous solution for protection against air. Because MEH-PPV is insoluble in water, such sample preparation guarantees that MEH-PPV chains do not mix with the cap polymer. We found that this "host matrix free" environment results in substantially stronger fluorescence spectral diffusion than that observed for conjugated polymer single chains embedded into polymer matrices. The average spectral diffusion range was 500 cm^{-1} , and the maximum registered value reached 1100 cm^{-1} , which is ~ 6 times larger than the values reported before. We analyzed spectral diffusion by observation of temporal evolution of the fluorescence intensity, the position of the maximum, and the width of fluorescence spectra. We propose that the transition energy shifts are caused by the differences of the London dispersive forces in slightly different polymer chain conformations. Such conformational changes are possible even at low temperatures because the MEH-PPV single chains in our samples have more freedom for fluctuations than in the usual "in host" arrangement.

1. Introduction

Single-molecule spectroscopy (SMS)^{1–3} allows the study of fluorescence properties of individual molecules. In this technique, only one molecule serves as a sample, allowing the possibility of avoiding ensemble averaging which is always present in spectroscopy of solutions or films. SMS has been successfully applied to conjugated polymers,² the organic semiconductors showing a great potential for various applications due to their electronic, optical, and topological properties. There is an important difference between a single chromophore (dye molecule) and a single chain of a conjugated polymer. First, a single polymer chain is not a single quantum system. A singlet excited state in a conjugated polymer chain (exciton) is localized on a small part of the chain^{4,5} often called the spectroscopic unit or chromophore. The spectroscopic unit length depends on the level of chemical and geometrical disorder and temperature.⁴ The typical spectroscopic unit length is ~ 5 – 9 monomer units,⁴ which is small in comparison with polymer chain length, which can be as large as 1000 monomer units for high-molecular weight molecules. Therefore, a single polymer chain consists of many (~ 100) weakly coupled chromophores (spectroscopic units) responsible for light absorption and emission. So, the "single chromophore level" is not reached by observing single polymer chains. However, due to downhill energy relaxation, only states close to the bottom of the excited-state manifold participate in fluorescence.⁶ Therefore, the relaxation process limits significantly the amount of chromophores contributing to the fluorescence spectrum. Thus, fluorescence properties of the whole polymer chain are mostly determined by properties of those specific segments often called "exciton funnels". This exciton "funneling" to specific emitting traps is the key issue

for application of the single-molecule spectroscopy technique to conjugated polymers.

Fluorescence intensity fluctuations^{1,7} ("blinking effect") have been observed in many systems, e.g., in single molecules (SMs) of organic dyes, biological complexes, and semiconductor quantum dots.⁸ The simplest explanation for the fluorescence blinking effect is that the molecule temporarily goes to a long-lived "dark" state (e.g., triplet state) where it cannot fluoresce. The phenomenon of fluorescence blinking has also been demonstrated for several conjugated polymers with high molecular weights containing hundreds of spectroscopic units^{6,9} and even for larger polymer clusters.¹⁰ The effect has been explained^{6,7} using the above-mentioned concept of exciton funneling. Emission from the exciton funnel can be quenched (e.g., by a closely situated quencher), resulting in fluorescence blinking of the whole polymer chain. The nature of the quencher and quenching mechanisms are not fully understood yet. Even for dye molecules such as Rh6G, the process of blinking and photobleaching is very complicated, involving several excited species and photochemical products.¹¹ Among possible candidates for quenching species are the charged species and triplet states.^{6,7,12} Recent experiments on charge injection and photo-oxidation in single MEH-PPV molecules showed that long-lived (seconds and tens of seconds) dark states do involve charged species.^{13,14}

It is generally agreed that polymer conformation plays an important role in blinking behavior. Conformation (or chain topology) determines the physical size of individual polymer molecules and influences the energy migration over the molecule. Polymer conformation can be controlled to a certain extent by changing solvents used for deposition onto a substrate.⁹ In our previous experiments, we have demonstrated the blinking effect to be present in MEH-PPV [soluble type of poly(phenylene vinylene)] single molecules also at low temperatures. We

* To whom correspondence should be addressed. E-mail: ivan.scheblykin@chemphys.lu.se.

did not observe any substantial difference between blinking at 300, 77,¹⁵ and 15 K.¹⁶ However, the efficiency of energy transfer toward the lowest-energy state must be much smaller at the cryogenic temperatures due to exciton trapping in local energy minima. We proposed the model of “direct quenching” when energy transfer to a single energy funnel is not necessary for fluorescence blinking. Direct quenching occurs when the quenching radius is comparable to the physical size of the polymer nanoparticle.¹⁵

Besides the fluorescence intensity, fluorescence spectra of single molecules also have a tendency to fluctuate over time.^{3,17} Spectral fluctuations at room temperature are usually attributed to thermal fluctuations of the environment, chromophore photoisomerization, or photochemical modification of the molecular system. We refer here to spectral fluctuations of dye molecules,^{17,18} small molecular ensembles (dendrimers),¹⁹ light-harvesting antennae,²⁰ and conjugated polymers.²¹ In those room-temperature studies, fluorescence spectra shifts as large as 200–1000 cm^{-1} were observed. Spectral and intensity fluctuations were also observed in semiconductor single quantum dots (QD).²² Moreover, it was shown that these two processes are correlated. Blinking in QD is the result of QD ionization and Auger electron–exciton (or hole–exciton) energy transfer. Therefore, the blinking process is accompanied by a strong change in the local electric field, leading to shifts of the fluorescence spectrum.⁸ In fact, the term “spectral diffusion” is more known in relation to low-temperature single-molecule and site selective spectroscopy of small molecules embedded into special matrices (Shpol’skii matrices). For such systems, photoinduced jumps of very narrow lines of fluorescence excitation spectra were observed.¹ The magnitude of these jumps is usually not more than a few inverse centimeters. The reason for such spectral diffusion is molecular transitions between two or more quasi-equilibrium positions in Shpol’skii matrices. Light-harvesting photosynthesis antennae have been studied by SMS methods at low temperatures. This is a molecular ensemble of tens of chromophores coupled to each other by resonance dipole–dipole interaction.

Different realizations of energetic disorder result in different exciton manifolds^{23,24} which were experimentally observed as different fluorescence²⁰ and fluorescence excitation spectra²⁵ for individual complexes. Thermal and photoinduced fluctuations of the energetic disorder were nicely observed as jumps in fluorescence excitation spectra at low temperatures.²⁵

Recently, a detailed study of single-molecule fluorescence spectral transients of MEH-PPV and MeLPPP [ladder type of poly(*p*-phenylene)] conjugated polymers at low temperatures was published.²⁶ The authors observed very narrow lines ($\text{fwhm} = 20 \text{ cm}^{-1}$) in fluorescence spectra for both polymers and spectral diffusion in the range of 20–200 cm^{-1} . Polymer chains in those studies were embedded in a nonfluorescent polymer host matrix. It was a surprise to see almost 1 order of magnitude stronger spectral diffusion in MEH-PPV molecules in our experiments at 15 K.²⁷ We attributed such a dramatic difference from the literature data to the “host matrix free” environmental conditions of MEH-PPV molecules under study, which allow them to have substantial conformational changes even at 15 K. In this work, more details of the spectral diffusion will be presented. Different spectroscopic characteristics of SM fluorescence spectra and their distributions will be discussed in relation to the spectral diffusion effect. We will also search for correlations between different spectral parameters of polymer single molecules. Possible origins for conformational fluctuations at cryogenic temperatures will be discussed.

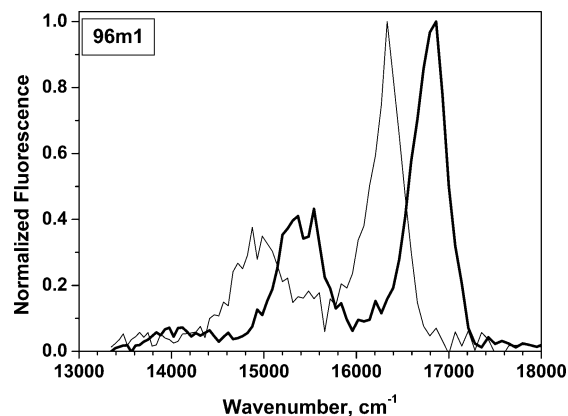


Figure 1. The most red-shifted and the most blue-shifted fluorescence spectra of the same single molecule obtained with an acquisition time of 0.3 s.

2. Experimental Section

Single molecules of poly[2-methoxy-5-(2'-ethylhexyloxy)-1,4-phenylene vinylene] (MEH-PPV, $M_n = 106\,000$, $M_w = 805\,000$, polydispersity of 7.6, American Dye Source, Inc.) were investigated with a wide field fluorescence microscope. Fluorescent light was collected with an Olympus objective lens (LCPlanFL60X, NA 0.7). The image was detected with a Cascade 512F CCD camera (Photometrics). MEH-PPV was spin-coated from a low-concentration toluene solution onto a Si/SiO₂ substrate. Then a cap layer of poly(vinyl alcohol) was spin-coated from a 1% aqueous solution to increase the sample photostability. During all experiments, the sample was kept in a vacuum (10^{-3} Torr or better) in a cryostat. The molecules were excited by a CW Ar ion laser at 514 nm. The frame acquisition time was 0.1–0.3 s, depending on excitation conditions, and the total measurement time of fluorescence time transients was 150–300 s. The typical excitation power density used in experiments was $\sim 300 \text{ W/cm}^2$.

Imaging of the polymer molecules and recording of their fluorescence spectra were carried out simultaneously by using holographic grating (Edmund Optics, 70 lines/mm) placed in front of the CCD camera. The distance between the CCD chip and the grating was such that the zero order and first order of the diffraction appeared on the CCD chip at the same time. The zero order gave an image, and the first order gave a spectrum. The advantage of this registration scheme was that it contained no slits and any other additional optics that could reduce the light collection efficiency. Fluorescence intensity transients were obtained by monitoring zero-order diffraction images of SMs. No corrections of the spectral sensitivity of the CCD camera were applied. A time of 0.3 s was needed to acquire a spectrum of a single MEH-PPV molecule with a good signal-to-noise ratio with an instrumental response function having a fwhm of $\approx 180 \text{ cm}^{-1}$ (6 nm). Fluorescence measurements were performed at 15 K.

The fluorescence spectrum of MEH-PPV exhibits a pronounced vibronic sub-band (ca. 1500 cm^{-1} , Figure 1) formed by several vibrational modes corresponding to C–C and C=C stretching.²⁸ To obtain quantitative characteristics of fluorescence spectrum of a SM, the initial spectrum was fitted with a sum of two Lorentzians. Positions of the peaks, their widths, and their amplitudes were independent fitting parameters. As the results of the fitting procedure, the above-mentioned parameters as functions of time and their time-averaged values were obtained (see Figure 2). Fitting of the spectra by the model function was necessary because of a quite low signal-to-noise

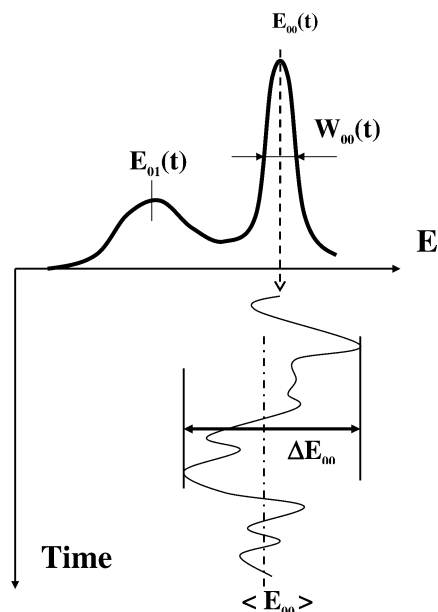


Figure 2. Characterization of fluorescence spectral diffusion.

ratio for molecules with weak fluorescence. This routine provided good reliability for the derived spectral characteristics even for quite noisy spectra. The following time-dependent parameters were calculated: $E_{00}(t)$ and $E_{01}(t)$, energies of the maxima of the first and second Lorentzian corresponding to the 0–0 and 0–1 fluorescence peaks, respectively; and $W_{00}(t)$, full width at half-maximum of the 0–0 peak. The fluorescence intensity $I(t)$ of the molecules was measured as the integrated signal from the zero order of diffraction from the grating. The following time-averaged parameters were calculated: $\langle E_{00} \rangle$, the average position of the 0–0 peak; $\langle W_{00} \rangle$, the average width of the 0–0 peak; $\Delta E_{00} = \max[E_{00}] - \min[E_{00}]$, spectral diffusion range; $\delta F = \Delta F/I_{\max}$, the maximum relative fluctuation of the fluorescence intensity, where ΔF is the maximum increase in fluorescence intensity; and I_{\max} , the maximal fluorescence intensity detected during the measurement. Thus, we take into account the upward intensity change only. Such a definition of δF allows us to characterize intensity fluctuations realistically, excluding the influence of photodegradation.¹⁶ For on–off blinking, $\delta F = 1$; for constant intensity or continuous decay, $\delta F = 0$. Each investigated molecule had its identification label (e.g., 96m1, 56m1). These labels are shown in all the graphs presented in the paper. It allows readers to follow a particular molecule through different graphs.

3. Results and Discussion

3.1. Averaged Spectral Position and Spectral Diffusion Range. The time dependence of the spectral position of 0–0 and 0–1 vibronic peaks is presented in Figure 3 for one molecule. Note that when the molecule is in the “off state” (fluorescence intensity is close to zero), the peak positions have no value. It can be seen that the drifts of positions of the two peaks are almost ideally correlated. But these positions were independent parameters during the fitting procedure. Therefore, this correlation is indisputable evidence that the spectral drifts do take place. This correlation shows that fitting errors are small compared to the observed spectral diffusion.

Examples of two “instant” spectra of a single molecule with an exposure time of 0.3 s are shown in Figure 1. The two spectra correspond to the most “red” and the most “blue” spectral positions observed during the experiment with this particular

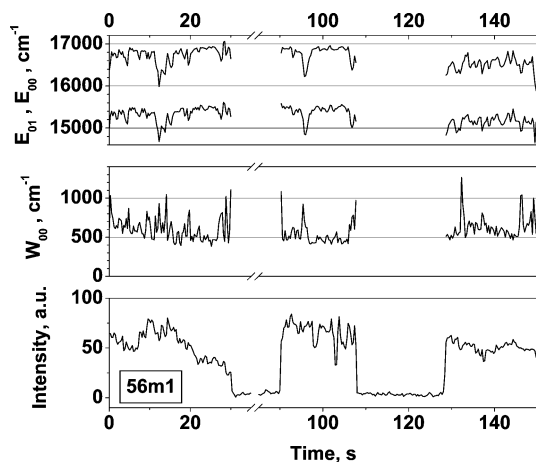


Figure 3. Time transients of fluorescence intensity (bottom panel), spectral width of the 0–0 band (middle panel), and positions of 0–0 and 0–1 vibronic bands (top panel) for the same molecule.

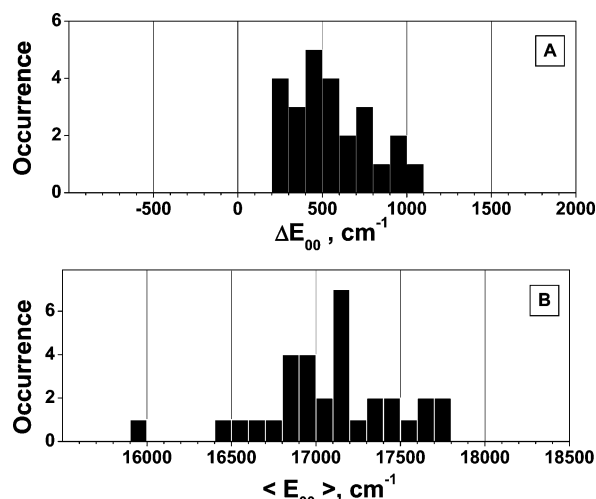


Figure 4. Histograms of the spectral diffusion range (A) and the time-averaged spectral position of the 0–0 vibronic band (B) for different molecules.

molecule. The spectral shift between these two positions (spectral diffusion range ΔE_{00} ; see the Experimental Section) is 500 cm^{-1} . Different molecules show different spectral diffusion ranges. A histogram of ΔE_{00} for different molecules is shown in Figure 4A. The maximal observed drift exceeded 1000 cm^{-1} . The average value of the spectral diffusion range was 500 cm^{-1} .

Typically, for most of the time, the position of a spectrum shows quite small fluctuations around its average. Large spectral fluctuations such as at $t = 12, 95$, and 108 s in Figure 3 happen quite seldom. For the molecule presented in the figure, the standard deviation of E_{00} is 200 cm^{-1} and the diffusion range $\Delta E_{00} = 1100 \text{ cm}^{-1}$. Any model, which we will be using for explaining the observed spectral diffusion, has to be capable of describing even the large spectral shifts. That is why the parameter ΔE_{00} instead of the standard deviation of E_{00} was chosen to characterize spectral diffusion.

Average positions of 0–0 peaks ($\langle E_{00} \rangle$) obtained by averaging $E_{00}(t)$ over the whole measuring time (usually 150 s) were also found to be very different for different molecules. A histogram of $\langle E_{00} \rangle$ is presented in Figure 4B. The distribution of $\langle E_{00} \rangle$ was very broad. The spectral difference between the “reddest” and the “bluest” molecule was as large as 1800 cm^{-1} . The width of this distribution was $\sim 800 \text{ cm}^{-1}$. These results are in agreement with the literature data.^{29,30} It is interesting to see that the spectral

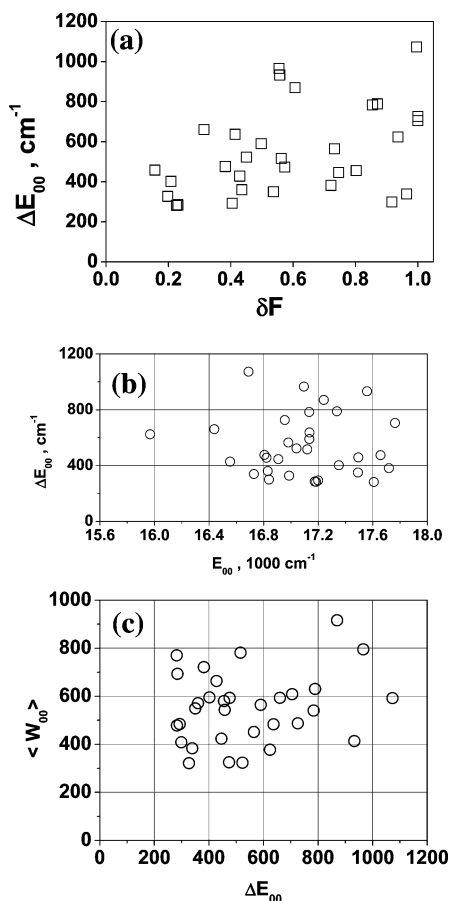


Figure 5. Averaged characteristics of fluorescence spectra of single molecules, with one point at each graph corresponding to a molecule. (a) Spectral diffusion range vs the maximum relative fluctuation of the fluorescence intensity. (b) Spectral diffusion range vs the average position of the 0–0 peak. (c) Average width of the 0–0 peak vs the spectral diffusion range.

diffusion range ΔE_{00} reaches the values which are ~ 2 times less than the width of the $\langle E_{00} \rangle$ distribution. This is also illustrated in Figure 5b, where the distance between each grid line is 400 cm^{-1} . We can conclude that a single molecule does not pass the full configuration space during the measurement time.

3.2. Spectral Drift and Blinking. Fluorescence intensity fluctuations (or blinking) were observed for the most part of the examined molecules. The detailed study of intensity fluctuations at low temperatures in MEH-PPV molecules has already been published.^{15,16} Note that the presence of the blinking effect makes our results differ from those obtained for MEH-PPV in a host polymer matrix.^{26,31} Only rare events of blinking were reported in these papers (see the comparison of the experimental data in section 3.4).

A correlation between fluorescence intensity and spectral position has been observed for semiconductor quantum dots.⁸ The authors showed that the fluorescence spectrum always shifts after the quantum dot stayed in the off state. Abrupt fluorescence intensity changes were accompanied by spectral changes in short chains of conjugated polymer dioctyloxy PPV that consisted of only 24 monomer units (four to five chromophores).³² The rodlike structure of the chains resulted in almost no energy transfer between chromophores in this polymer. Bleaching of independently emitting chromophores led both to intensity drops and shifts of the fluorescence spectrum.

In the following, we will search for correlation between the spectral position and fluorescence intensity in our data. A

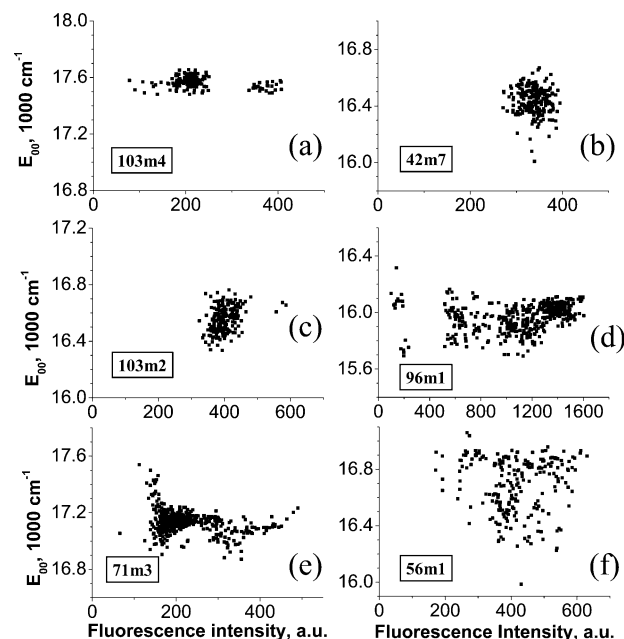


Figure 6. Spectral position vs fluorescence intensity. Each plot represents one single molecule. Data when the fluorescence intensity was close to zero are not shown. Identification labels of molecules are shown in the frames.

pictorial form of data presentation is used in Figure 6. It is made up of the scatter graphs of spectral position $E_{00}(t)$ versus fluorescence intensity $I(t)$ for six molecules. For the sake of clarity, the vertical axis (spectral position) has the same scale for all the plots (full scale = 1200 cm^{-1}). These graphs demonstrate how individual the behavior of SM fluorescence is. For example, molecule (a) shows obvious blinking behavior between two levels of 200 and 400 intensity units. However, this blinking molecule had almost no spectral diffusion (range of spectral drift was less than 200 cm^{-1}). In contrast to that, molecules (b) and (c) possessed substantial spectral drift (range was $\sim 300\text{--}600 \text{ cm}^{-1}$) and small intensity fluctuations. Molecules d–f demonstrated a complicated behavior combining spectral and intensity fluctuations.

One can also look at a time evolution of the spectral position and fluorescence intensity for a single molecule. The unaided eye cannot really see correlations between the two parameters in the examples shown in Figures 3 and 7A,B. Indeed, from Figure 3 we can see that there are considerable intensity changes accompanied by no spectral drifts, and vice versa. To characterize linear correlation of the two data sets, the standard Pearson's coefficient r is usually employed.³³ It takes values from -1 to 1 , where in the absence of noise $|r| = 1$ corresponds to a strict linear relationship (with a positive first coefficient for $r = 1$ and a negative for $r = -1$) between the data sets. The $|r| < 1$ case corresponds to the intermediate cases with other types of relationships or a complete absence of such. However, the kind of correlation that is of interest to us may occur on time scales much shorter than the whole measurement time. To analyze such correlations, we used a modified, "local" Pearson's r defined as follows:

$$r_{\Delta t}(t) = \frac{\langle [A(t) - \langle A \rangle_{\Delta t}] [B(t) - \langle B \rangle_{\Delta t}] \rangle_{\Delta t}}{\sqrt{\langle [A(t) - \langle A \rangle_{\Delta t}]^2 \rangle_{\Delta t}} \sqrt{\langle [B(t) - \langle B \rangle_{\Delta t}]^2 \rangle_{\Delta t}}}$$

where the averaging is done over the time interval $(t - \Delta t/2, t + \Delta t/2)$. By using different averaging intervals Δt , we can analyze the correlations on different time scales. The typical

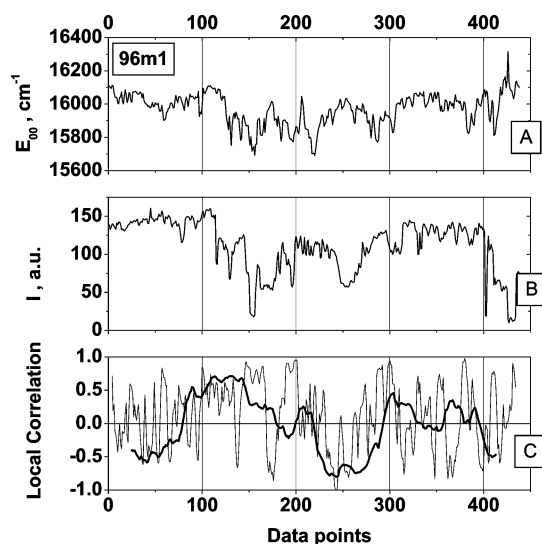


Figure 7. (A and B) Time transients of the spectral position (E_{00}) and the fluorescence intensity. (C) Local correlation coefficient between spectral position and intensity calculated for 50 data points (thick line) and 8 data points (thin line).

result of such analysis is shown in Figure 7. Data points were equidistant in time (0.3 s), so numbers of data points were used instead of time. The two top plots show time evolution of E_{00} and W_{00} . The bottom plot contains $r_{50}(t)$ and $r_8(t)$, Pearson's r calculated for 50- and 8-data point time windows, respectively. Oscillation of the coefficients from -1 to $+1$ is an indication of the absence of correlation between the fluorescence intensity and spectral position of single molecules at those frequencies. The correlation coefficient for the whole data sets was also calculated for each molecule. Its average value over different molecules was very close to zero. Time-averaged characteristics of spectral diffusion (ΔE_{00}) and intensity blinking (δF) for different molecules also do not show any noticeable correlation. A scatter graph of ΔE_{00} versus δF demonstrates a quite uniform distribution of the data points (Figure 5a). These experimental observations limit possible mechanisms of spectral diffusion.

3.3. Spectral Width. The value of spectral width W_{00} was more sensitive to the signal-to-noise ratio than the spectral position E_{00} . To avoid artifacts related to the fitting procedure, spectra showing a good signal-to-noise ratio were selected to determine the spectral width. The time-averaged values of the width $\langle W_{00} \rangle$ against ΔE_{00} for different molecules are presented in Figure 5c. The average spectral width was very different for different molecules, ranging from 300 to 1000 cm^{-1} . The fact that the width can be so different shows that it cannot be the intrinsic width of the single chromophore fluorescence. One can see that there are molecules with narrow spectra ($\langle W_{00} \rangle < 450$ cm^{-1}) showing a spectral diffusion range ΔE_{00} from 300 to 950 cm^{-1} . For a substantial part of the molecules, the averaged width and spectral diffusion range were quite close in magnitude. Spectral width, as well as spectral position, was found to fluctuate over time (Figure 3). These fluctuations are illustrated in the scatter graph in Figure 8, where values of $W_{00}(t)$ versus spectral position $E_{00}(t)$ are depicted for three different molecules. Graph (c) shows one extreme case when the spectrum was fluctuating almost without a spectral width change. Graph (b) demonstrates another extreme case in which the spectral width fluctuations are even larger than the fluctuations of spectral position. However, often a clear correlation between sharp fluctuations of spectral width and rapid changes of the spectral position (maximum of the spectral position derivative) was observed. Indeed, in Figure 3 all the substantial peaks in $W_{00}(t)$

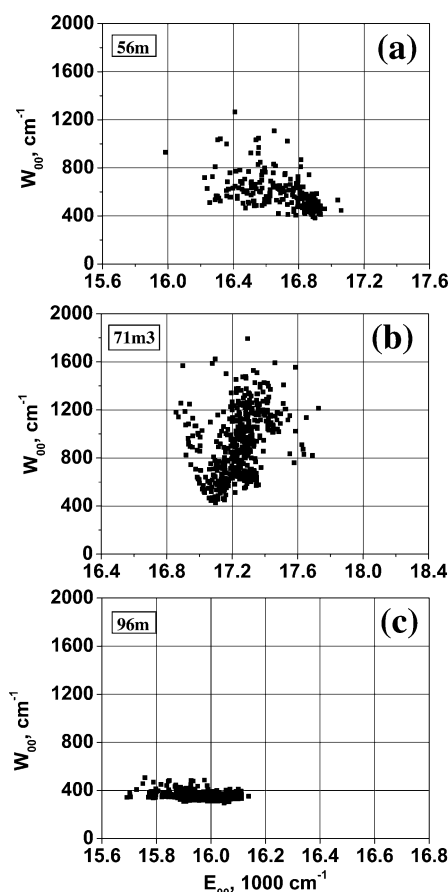


Figure 8. Spectral width vs spectral positions for three different molecules. The acquisition time for each point was 0.3 s.

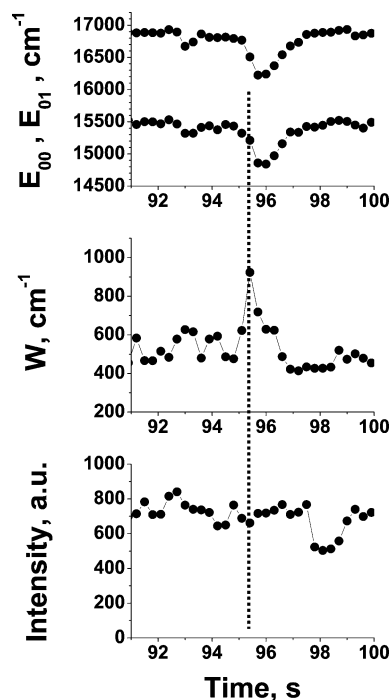


Figure 9. Same as Figure 3 but the time scale is expanded around $t = 95$ s.

correspond to fast spectral movement of the fluorescence band (see Figure 9 for clarity). This indicates that large values of the width (like 1000 cm^{-1}) probably originate from poorly resolved spectral diffusion. We cannot exclude the possibility that there may be a spectral diffusion with a characteristic time scale much

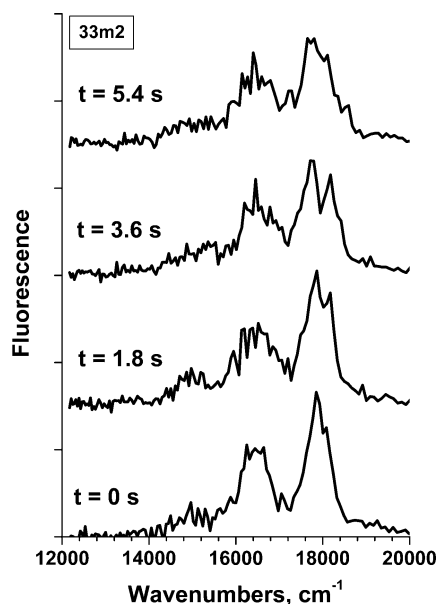


Figure 10. Molecule with a temporary double-peak spectral structure. The acquisition time for each spectrum was 0.3 s. The points of time when the spectra were measured are shown.

shorter than the temporal resolution of the experiment. Such fast spectral diffusion can be the source of the line broadening.

Besides large fluctuations in spectral width, for some molecules temporary double-peak spectra were observed. Of course, such spectral shape cannot be described by the model function used for processing of the spectra (see the Experimental Section). However, these cases were seldom and, therefore, did not influence the overall statistics. An example of such behavior is shown in Figure 10. Note that this double-peak structure was observed in several spectra obtained consecutively. That is why it was not the result of a temporally unresolved jump of the spectrum from the initial to its final position. Obviously, the double-peak spectrum means that the particular molecule has at least two emitting sites with different energies, or it is changing between these two states back and forth faster than the temporal resolution of the experiment (0.3 s). Although such clear double-peak structure was observed quite seldom, it shows that the broad spectra (with a width of $>500\text{ cm}^{-1}$) may have unresolved internal structure.

3.4. Comparison with the Literature Data. It is interesting to compare the experiments of different groups carried out on MEH-PPV single molecules at low temperatures (Table 1). One can see that the results reported in this work are quite different from the results of previous studies. The most important difference is in the magnitude of spectral diffusion range ΔE_{00} .

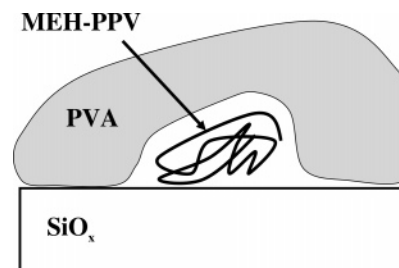


Figure 11. Schematic illustration of a MEH-PPV chain in a caged matrix free environment.

We observed spectral fluctuations at least 6 times larger than those reported previously. The observed value of spectral drift at 15 K is actually as large as the one for MEH-PPV at room temperature.²¹

The only difference between our sample and the samples studied in the other works cited in the table is the different environmental conditions of MEH-PPV chains. In the papers by other authors, MEH-PPV chains were imbedded in a nonfluorescing host polymer matrix, dissolved in the same solution. In our case, the MEH-PPV molecules were spin-coated directly from solution in toluene without using any matrix polymer. Afterward, the substrate with the attached MEH-PPV chains was coated with a layer of PVA to increase the photostability of the sample in a manner similar to that described in ref 21. We point out that MEH-PPV is insoluble in water, the solvent that was used for dissolving the cap polymer. A schematic illustration would be to imagine a MEH-PPV chain enclosed in a “cave” formed by PVA (Figure 11). Moreover, the conformation of polymer chains deposited directly from diluted solution must be different because there is no matrix around during the deposition process to prevent the MEH-PPV chain from reaching its favorable conformation. Such an “in-cave” chain has much more freedom to change its conformation than a chain fixed in a host polymer matrix. As will be shown below, conformational changes are the most probable reasons for the observed spectral fluctuations.

The line width observed in our experiments is larger than what has been reported in the literature. The spectral width in our experiments ranges from 300 to 1000 cm^{-1} for different molecules. The fact that the width can be so different for different molecules shows that it cannot be the intrinsic width of the single chromophore fluorescence. We also have direct evidence that temporal unresolved spectral diffusion makes a strong contribution to fluorescence line broadening (section 3.3). Contrary to our study, very narrow fluorescence spectra have been observed for short chains (70 monomer units) of a conjugated polymer MeLPPP³⁴ in a polystyrene host matrix. This polymer has a very rigid laddertype structure and contains

TABLE 1: Fluorescence of Single Chains of Conjugated Polymers at Low Temperatures

	Ronne et al. ²⁹	Yu and Barbara ³¹	Schindler et al. ²⁶	this paper
temperature (K)	~20	~20	~5	~15
solvent	toluene	toluene, chlorophorm	toluene	toluene
polymer matrix	PMMA	PMMA, polystyrene	polystyrene	none
cap layer	none	none	none	PVA
M_n (polydispersity)	? (?)	450000 (2.2)	200000 (?)	108000 (7.6)
fluorescence blinking	no data	sometimes	sometimes	yes
spectrum acquisition time (s)	90	60	2	0.3
main band spectral width (cm^{-1})				
minimal	200	no data	~10	300 ^a
average	400	300	?	500 ^a
maximal	900	no data	~200	1100 ^a
spectral diffusion range ΔE_{00} (cm^{-1})	no data	not observed	50/160	300/1100

^a Without correction on IRF = 180 cm^{-1} .

not more than 10 chromophores (spectroscopic units). The observed fluorescence spectra consisted of several distinct narrow peaks attributed to emission from single chromophores with different energies. The smallest line width reported in that work was 2.5 meV, or 20 cm⁻¹. It was a surprise that equally narrow lines were observed for high-molecular weight MEH-PPV single chains in the polystyrene matrix by the same research group.²⁶ Those narrow spectra also exhibited spectral diffusion (Table 1). A long acquisition time (60 s compared to 2 s in ref 26) could be the reason those narrow lines were not observed in ref 31, where MEH-PPV was studied under very similar conditions. The spectral width was reported to be around 300 cm⁻¹ at 20 K in that study. The authors also observed multipeak spectra similar to the ones presented in Figure 10 and attributed them to emission from independent chromophores.

3.5. Excited-State Energies of a Conjugated Polymer Single Chain. A single chain of a conjugated polymer can be imagined as an ensemble of many individual chromophores, spectroscopic units. The number of chromophores is on the order of 100. Each chromophore has its own excited-state energies. An illustrative schematic way would be to imagine a polymer chain having 100 excited states of different energies (if vibrational states are not taken into account) localized on different places of the chain. The energies of the excited states of a chromophore depend on the exciton delocalization length and interaction with the environment. Below we consider these factors in detail.

1. Exciton Delocalization Length (chromophore length). Experiments with oligomers with different lengths and quantum chemistry calculations have shown that the vertical 0–0 transition energy of a chromophore as a function of the number of monomer units can be expressed as

$$E_{00}^v(N) = E_0 + 2\beta \cos\left(\frac{\pi}{N+1}\right) \quad (1)$$

where $E_0 = 34\,400$ cm⁻¹ and $\beta = -8800$ cm⁻¹ for MEH-PPV in chloroform.³⁵ Equation 1 gives, e.g., $E_{00}^v(5) - E_{00}^v(10) = 1645$ cm⁻¹. One can see that the effect of the different length is quite large. This means that differences in conjugation lengths of emitting chromophores can account for variation in average observed spectral positions (Figure 4B; see also ref 29).

2. "Solvent Effects". Energy level shifting due to so-called solvent effects^{36,37} is caused by the changes in the stationary dipole moment and/or polarizability of a chromophore upon electronic transition. Since the stationary dipole is negligible in MEH-PPV, the main effect is due to changes in polarizability. The magnitude of the transition energy shift due to different polarizabilities in ground and excited states can be evaluated by considering a dispersive interaction between two chromophores. The latter can be estimated with the London formula³⁸

$$E \approx -\frac{3}{2} \frac{\Delta E_A \Delta E_B}{\Delta E_A + \Delta E_B} \frac{\alpha'_A \alpha'_B}{R^6} \quad (2)$$

where ΔE_A and ΔE_B are the average transition energies, α'_A and α'_B are the polarizabilities of the chromophores, and R is the distance between them. As an estimate of the average transition energy, half of the ionization energy can be used for conjugated polymers. Assuming that the chromophores are identical and using eq 2, we obtain

$$\Delta E = E_{\text{medium}} - E_{\text{vacuum}} = -\frac{3}{8} I \frac{\alpha'_g \Delta \alpha'}{R^6} \quad (3)$$

for the spectral shift of a chromophore upon moving it from vacuum to a distance R from the other chromophore, where an I of $\approx 50\,000$ cm⁻¹ (ref 39) is the ionization energy of MEH-PPV, a $\Delta \alpha'$ of 500 Å³ (ref 40) is the change in polarizability upon electronic transition, and α'_g is the ground-state polarizability of a chromophore. In this study, we applied quantum chemistry calculations to evaluate α'_g . We used the Gaussian 03 program package for calculating the polarizability of two PPV-type oligomers composed of two and four phenylene rings by Hartree–Fock and density functional theory using basis sets with and without polarization functions. We conclude that the ground-state polarizabilities for the two- and four-unit oligomers are 25 and 100 Å³, respectively. Assuming $\alpha'_g = 100$ Å³ and $R = 10$ Å, we obtain a ΔE of ≈ 1000 cm⁻¹ from eq 3 for the spectral shift. Changing the distance between the chromophores from 10 to 9 Å would lead to a further red shift of almost 900 cm⁻¹.

$\Delta \alpha'$ of MEH-PPV may also cause the energy shifts due to interaction with the stationary dipoles of PVA. We used Gaussian 03 to evaluate the dipole moment of PVA and found that changing the distance between MEH-PPV and PVA segments from 10 to 9 Å would lead to a spectral shift of ~ 80 cm⁻¹, which is smaller than the above estimate for two MEH-PPV segments by 1 order of magnitude.

We point out that in a very recent study of fluorescence spectra of individual short polymer chains with a known amount of emitting chromophores it was suggested that interaction with the environment rather than the chromophore length is the leading factor determining the position of 0–0 lines in the fluorescence spectra.⁴¹ In this work, we have identified the London's dispersive forces between different parts of a polymer chain as the most important part of the chromophore, environment interaction.

3. Resonance Interaction between Chromophores. Two neighboring chromophores interact with each other via interaction between exciton transition dipoles. It can change the transition energy by an amount comparable to the interaction strength. Various computational methods have been used to calculate the resonance interaction in conjugated polymers.^{5,42} Resonance interaction can reach up to 1000 cm⁻¹ for closely packed polymer segments with an intersegment distance of 5 Å.⁴² However, it has a much weaker distance dependence (R^{-3}) in comparison with that for dispersive forces (R^{-6}). Therefore, the contribution of the resonance interaction to the energy shift due to changes of the distance between two chromophores will be much smaller than that from the dispersive forces discussed above.

3.6. Reasons for Temporal Spectral Fluctuations. As we have shown, the most important factors determining the energy level of a chromophore is its length and its interaction with other chromophores of the same polymer chain. To explain the spectral diffusion, we should assume that the exciton level manifold is changing over time by some mechanisms.

Because of the complexity of the systems, it is not easy to form conclusions about the mechanisms. Most probably, for different molecules the main factors can be different, too. However, all the possible explanations can be split into two groups by involving and not involving photochemical damage of the polymer.

By photochemical damage we assume permanent or temporal bleaching of segments of the polymer chain and/or photogeneration of different types of fluorescence quenchers. Temporal or permanent bleaching of chromophores of different energies contributing to the fluorescence will change the fluorescence

spectrum. To illustrate the idea, let us imagine a chain having two energy funnels of the same emission intensity but slightly different in energy. Then, quenching of either will shift the fluorescence spectrum. If the particular chromophore being quenched remains a funnel for excitons, then the total fluorescence intensity should be reduced 2 times. However, it is possible that the chromophore being in the dark state does not work as an exciton funnel anymore. In that case, fluorescence intensity will not undergo substantial changes. Of course, it can be not only two but also three or more chromophores contributing to the emission. The spectral diffusion range maximum value in this model is equal to the energy difference between the most red and the most blue chromophore. Another possible scenario is that after bleaching (quenching) of the funnel, another chromophore takes over and becomes a funnel. The latter was used to explain spectral changes observed in MEH-PPV chains at room temperature²¹ when fluorescence spectra were steadily shifting to the blue, indicating the steady bleaching of the reddest chromophores of the polymer chain.

We cannot exclude the possibility that photochemical damage plays a role in our system, too. However, it is unlikely that this is the only factor and the major factor. First, single molecules of MEH-PPV at low temperatures exhibit quite slow photobleaching in comparison to that at room temperature.²¹ Second, we did not observe any systematic drifts of the spectra toward shorter wavelengths. The spectra were fluctuating toward both sides from their average positions. This is a strong argument against that simple model in which the polymer chain is just “chopped” by photogenerated defects into smaller and smaller segments.

The third point to mention is the character of the spectral fluctuations. Indeed, sharp jumplike changes would be expected if exciton funnels become spontaneously photobleached. Contrary to that, a rather smooth spectral drift can be seen in Figure 9, where we have presented a “zoom in” of one of the large spectral fluctuation of molecule 56m1.

There is also a problem with the spectral diffusion range. If the spectrum shifts on 1000 cm^{-1} to the blue side, it would mean that all states with lower energies had been bleached. However, 1000 cm^{-1} is already almost 30% of the fwhm of the absorption spectrum, which is $\sim 3500\text{ cm}^{-1}$ at room temperature in solution.³⁵ Bleaching of such a large number of states will definitely result in a decrease in the fluorescence intensity regardless of the nature of the bleaching. However, as shown in section 3.2, no obvious correlation was observed between the spectral shift and the fluorescence intensity.

Another argument against the model of photochemical damage is that there is no solid ground to think that photochemistry is very different for MEH-PPV chains placed into the PMMA host matrix or covered by a PVA cap layer. Then the question is why strong spectral diffusion was not observed for MEH-PPV in PMMA and PS matrices.

All these arguments call for an alternative explanation for the large spectral diffusion observed in this work.

Let us consider the situation in which no photobleaching is involved. In this case, it should be assumed that the energy of the existing excited states is changing with time. Conformational change is a natural candidate to be the reason for this because chain conformation determines dispersion forces, intrasegment resonance interactions, and partially chromophore length distribution. Even quite small changes in conformation (see above) can lead to a substantial shift of the energy levels. However, if one takes into account the multistep exciton relaxation process, conformational fluctuations needed to account for the observed

fluctuations of the fluorescence spectra can be even smaller. Indeed, the excitation energy in our experiments is $19\,455\text{ cm}^{-1}$ (514 nm), while average emission maximum is $17\,000\text{ cm}^{-1}$. So, exciton loses $\sim 2500\text{ cm}^{-1}$ of energy during the relaxation process. This relaxation process includes also exciton migration over the polymer chain, because different states are localized at different segments of the chain. Due to many steps involved in the relaxation process, small changing of even a few levels of the exciton manifold may force the exciton to proceed to a very different final relaxed state.

The polymer chain topology can be changed due to temperature-induced fluctuations. However, these fluctuations must be very small at 15 K. Therefore, it is really questionable whether the thermal fluctuations are the main reason. Another source of energy, at least a part of which can be used for changing polymer conformation, is the excess energy (ca. 2500 cm^{-1}) coming from photoexcitation. It does not lead to real heating of the material because of the low rate of excitation events and the large number of degrees of freedom in the system. However, excess energy redistribution through vibrations needs some time. Just after the excitation event, the density of vibronic energy is leading to strong perturbation of the part of the polymer chain around the localization of the excited state. The in-cave MEH-PPV arrangement probably decreases the rate of vibration energy dissipation toward the environment (substrate and PVA layer) in comparison to placing MEH-PPV into a host polymer matrix. One of the mechanisms of light-induced conformational change can be a result of the difference between London forces in the ground and excited states. This difference results in mechanical tension during each period of excitation.

4. Conclusions

Large-amplitude spectral diffusion was observed for single molecules of conjugated polymer MEH-PPV at 15 K. The average spectral diffusion range was 500 cm^{-1} , and the maximum registered value was 1100 cm^{-1} . These values are at least 6 times larger than what has been previously reported for conjugated polymers at cryogenic temperatures. We analyzed the temporal evolution of the spectral maximum position, the width of the fluorescence spectra, and the fluorescence intensity. The fluorescence intensity and the spectral position for a single molecule were found to fluctuate in time without noticeable correlation. Also, no correlation was found between the spectral diffusion range and the amplitude of fluorescence intensity blinking, averaged characteristics measured for different single molecules. Temporal fluctuations of the single-molecule spectral width were attributed to temporally unresolved spectral diffusion. Evaluation of the spectral shifts due to the dispersive interaction between nearby chromophores of a coiled polymer chain shows that due to the strong distance dependence ($\propto R^{-6}$) of the interaction, small conformational fluctuations can lead to substantial shifts of the excited-state energies. Changing of the exciton level manifold due to changing of the dispersive forces during conformational fluctuations of the chain and the temporal photobleaching of exciton funnels are the main possible mechanisms of spectral diffusion. The first mechanism alone or a combination of the two can account for the observed large-amplitude spectral drifts. Photobleaching of the segments of the chain cannot alone account for the spectral diffusion. The most probable candidate for the driving force behind these conformational fluctuations is light excitation. By comparing our results with the literature data on conjugated polymer single molecules embedded in polymer host matrices, we conclude that the sample structure with matrix free MEH-PPV chains is

the key issue for the large observed spectral diffusion. MEH-PPV single chains in our samples have much more freedom for conformational fluctuations compared to the usual in-host molecule arrangement.

Acknowledgment. This work was financially supported by the STINT-DAAD program, the Swedish Research Council, the Knut&Alice Wallenberg Foundation, the Crafoord Foundation, and the Swedish Institute. We thank Villy Sundström and Arkady Yartsev (Chemical Physics, Lund University) for valuable discussions. We are also grateful to Christian von Borczyskowski and Frank Cichos for giving us the opportunity to use experimental equipment of the Department of Optical Spectroscopy and Molecular Physics and Group of Photonics and Optical Materials (Chemnitz University of Technology, Chemnitz, Germany), and useful discussions.

References and Notes

- (1) Orrit, M. *J. Chem. Phys.* **2002**, *117*, 10938–10946.
- (2) Kulzer, F.; Orrit, M. *Annu. Rev. Phys. Chem.* **2004**, *55*, 585–611.
- (3) Michalet, X.; Weiss, S. C. R. *Phys.* **2002**, *3*, 619–644.
- (4) Pope, M.; Swenberg, C. E. *Electronic Processes in Organic Crystals and Polymers*, 2nd ed.; Oxford University Press: New York, 1999.
- (5) Beenken, W. J. D.; Pullerits, T. *J. Phys. Chem. B* **2004**, *108*, 6164–6169.
- (6) Yu, J.; Hu, D. H.; Barbara, P. F. *Science* **2000**, *289*, 1327–1330.
- (7) Yip, W. T.; Hu, D. H.; Yu, J.; Vanden Bout, D. A.; Barbara, P. F. *J. Phys. Chem. A* **1998**, *102*, 7564–7575.
- (8) Neuhauser, R. G.; Shimizu, K. T.; Woo, W. K.; Empedocles, S. A.; Bawendi, M. G. *Phys. Rev. Lett.* **2000**, *85*, 3301–3304.
- (9) Huser, T.; Yan, M. *J. Photochem. Photobiol., A* **2001**, *144*, 43–51.
- (10) Scheblykin, I.; Zorinants, G.; Hofkens, J.; De Feyter, S.; Van der Auweraer, M.; De Schryver, F. C. *ChemPhysChem* **2003**, *4*, 260–267.
- (11) Zondervan, R.; Kulzer, F.; Kol'chenko, M. A.; Orrit, M. *J. Phys. Chem. A* **2004**, *108*, 1657–1665.
- (12) Osad'ko, I. S. *J. Exp. Theor. Phys.* **2003**, *96*, 617–628.
- (13) Park, S. J.; Gesquiere, A. J.; Yu, J.; Barbara, P. F. *J. Am. Chem. Soc.* **2004**, *126*, 4116–4117.
- (14) Gesquiere, A. J.; Park, S. J.; Barbara, P. F. *J. Phys. Chem. B* **2004**, *108*, 10301–10308.
- (15) Mirzov, O.; Cichos, F.; von Borczyskowski, C.; Scheblykin, I. G. *Chem. Phys. Lett.* **2004**, *386*, 286–290.
- (16) Mirzov, O.; Cichos, F.; von Borczyskowski, C.; Scheblykin, I. G. *J. Lumin.* **2005**, *112*, 353–356.
- (17) Lu, H. P.; Xie, X. S. *Nature* **1997**, *385*, 143–146.
- (18) Blum, C.; Stracke, F.; Becker, S.; Mullen, K.; Meixner, A. J. *J. Phys. Chem. A* **2001**, *105*, 6983–6990.
- (19) Hofkens, J.; Maus, M.; Gensch, T.; Vosch, T.; Cotlet, M.; Kohn, F.; Herrmann, A.; Mullen, K.; De Schryver, F. *J. Am. Chem. Soc.* **2000**, *122*, 9278–9288.
- (20) Rutkauskas, D.; Novoderezhkin, V.; Cogdell, R. J.; van Grondelle, R. *Biochemistry* **2004**, *43*, 4431–4438.
- (21) Huser, T.; Yan, M.; Rothberg, L. J. *Proc. Natl. Acad. Sci. U.S.A.* **2000**, *97*, 11187–11191.
- (22) Nirmal, M.; Dabbousi, B. O.; Bawendi, M. G.; Macklin, J. J.; Trautman, J. K.; Harris, T. D.; Brus, L. E. *Nature* **1996**, *383*, 802–804.
- (23) Mostovoy, M. V.; Knoester, J. *J. Phys. Chem. B* **2000**, *104*, 12355–12364.
- (24) Dempster, S. E.; Jang, S. J.; Silbey, R. J. *J. Chem. Phys.* **2001**, *114*, 10015–10023.
- (25) van Oijen, A. M.; Ketelaars, M.; Kohler, J.; Aartsma, T. J.; Schmidt, J. *Biophys. J.* **2000**, *78*, 1570–1577.
- (26) Schindler, F.; Lupton, J. M.; Feldmann, J.; Scherf, U. *Proc. Natl. Acad. Sci. U.S.A.* **2004**, *101*, 14695–14700.
- (27) Mirzov, O.; Pullerits, T.; Cichos, F.; von Borczyskowski, C.; Scheblykin, I. G. *Chem. Phys. Lett.* **2005**, *408*, 317–321.
- (28) Mulazzi, E.; Ripamonti, A.; Wery, J.; Dulieu, B.; Lefrant, S. *Phys. Rev. B* **1999**, *60*, 16519–16525.
- (29) Ronne, C.; Tragardh, J.; Hessman, D.; Sundstrom, V. *Chem. Phys. Lett.* **2004**, *388*, 40–45.
- (30) Yu, Z. H.; Barbara, P. F. *J. Phys. Chem. B* **2004**, *108*, 11321–11326.
- (31) Yu, Z. H.; Barbara, P. F. *J. Phys. Chem. B* **2004**, *108*, 11321–11326.
- (32) Wang, C. F.; White, J. D.; Lim, T. L.; Hsu, J. H.; Yang, S. C.; Fann, W. S.; Peng, K. Y.; Chen, S. A. *Phys. Rev. B* **2003**, *67*.
- (33) Press, W. H.; Teukolsky, S. A.; Vetterling, W. T.; Flannery, B. P. *Numerical Recipes in C: The Art of Scientific Computing*, 2nd ed.; Cambridge University Press: New York, 1992.
- (34) Muller, J. G.; Lemmer, U.; Raschke, G.; Anni, M.; Scherf, U.; Lupton, J. M.; Feldmann, J. *Phys. Rev. Lett.* **2003**, *91*.
- (35) Chang, R.; Hsu, J. H.; Fann, W. S.; Liang, K. K.; Chiang, C. H.; Hayashi, M.; Yu, J.; Lin, S. H.; Chang, E. C.; Chuang, K. R.; Chen, S. A. *Chem. Phys. Lett.* **2000**, *317*, 142–152.
- (36) Kumar, P.; Mehta, A.; Dadmun, M. D.; Zheng, J.; Peyser, L.; Bartko, A. P.; Dickson, R. M.; Thundat, T.; Sumpter, B. G.; Noid, D. W.; Barnes, M. D. *J. Phys. Chem. B* **2003**, *107*, 6252–6257.
- (37) Schwartz, B. J. *Annu. Rev. Phys. Chem.* **2003**, *54*, 141–172.
- (38) Atkins, P. W.; Friedman, R. S. *Molecular Quantum Mechanics*, 3rd ed.; Oxford University Press: New York, 1997; Chapter 12.5, pp 389–392.
- (39) Seki, K.; Asada, S.; Mori, T.; Inokuchi, H.; Murase, I.; Ohnishi, T.; Noguchi, T. *Solid State Commun.* **1990**, *74*, 677–680.
- (40) Gelinck, G. H.; Piet, J. J.; Wegewijs, B. R.; Mullen, K.; Wildeman, J.; Hadzioannou, G.; Warman, J. M. *Phys. Rev. B* **2000**, *62*, 1489–1491.
- (41) Schindler, F.; Jacob, J.; Grimsdale, A. C.; Scherf, U.; Mullen, K.; Lupton, J. M.; Feldmann, J. *Angew. Chem., Int. Ed.* **2005**, *44*, 1520–1525.
- (42) Beljonne, D.; Pourtois, G.; Silva, C.; Hennebicq, E.; Herz, L. M.; Friend, R. H.; Scholes, G. D.; Setayesh, S.; Mullen, K.; Bredas, J. L. *Proc. Natl. Acad. Sci. U.S.A.* **2002**, *99*, 10982–10987.